Geophysical Research Letters

RESEARCH LETTER
10.1029/2025GL115640

# A New Approach to Identifying and Analyzing Precipitation Events and Their Typical Lifecycles Over Conterminous United States

**Siyu Zhu[1], Guoqiang Tang[2], Songkun Yan[1], Yu Du[3], Yue Xu[4], Mofan Zhang[5], Mengye Chen[1], Huan Li[6], and Yang Hong[1]**

[1]School of Civil Engineering and Environmental Science, and HyDROS Lab at National Weather Center, University of Oklahoma, Norman, OK, USA, [2]State Key Laboratory of Water Resources Engineering and Management, Wuhan University, Wuhan, China, [3]School of Atmospheric Sciences, Sun Yat-sen University, and Southern Marine Science and Engineering Guangdong Laboratory (Zhuhai), Zhuhai, China, [4]School of Earth and Space Sciences, Institute of Remote Sensing and Geographic Information Systems, Peking University, Beijing, China, [5]Civil and Environmental Engineering, Stanford University, Stanford, CA, USA, [6]HUN-REN Balaton Limnological Research Institute, Tihany, Hungary

**Key Points:**

- A novel morphological method is developed to extract and analyze diverse precipitation events with improved accuracy and efficiency
- A robust lifecycle model is proposed to quantify precipitation evolution, capturing key phases of development, maturity, and dissipation
- The proposed method demonstrates high stability and consistency across three major precipitation data sets, ensuring broad applicability

**Supporting Information:**

Supporting Information may be found in the online version of this article.

**Correspondence to:**

G. Tang and Y. Hong,
guoqiang.tang@whu.edu.cn;
yanghong@ou.edu

**Citation:**

Zhu, S., Tang, G., Yan, S., Du, Y., Xu, Y., Zhang, M., et al. (2025). A new approach to identifying and analyzing precipitation events and their typical lifecycles over conterminous United States. *Geophysical Research Letters*, *52*, e2025GL115640. https://doi.org/10.1029/2025GL115640

Received 1 MAR 2025
Accepted 23 JUN 2025

**Author Contributions:**

**Conceptualization:** Guoqiang Tang, Yu Du, Mengye Chen, Yang Hong
**Data curation:** Siyu Zhu
**Funding acquisition:** Yang Hong
**Methodology:** Siyu Zhu, Guoqiang Tang, Yu Du, Yue Xu, Mofan Zhang, Mengye Chen, Yang Hong
**Project administration:** Guoqiang Tang, Yang Hong
**Software:** Siyu Zhu, Guoqiang Tang, Songkun Yan, Yue Xu
**Supervision:** Guoqiang Tang, Yang Hong
**Validation:** Guoqiang Tang, Songkun Yan
**Visualization:** Siyu Zhu, Songkun Yan



**Abstract** Precipitation is a key driver of the global water cycle and energy circulation, yet its complex formation and dynamic lifecycle make both observation and simulation challenging. Tracking precipitation events and analyzing their lifecycle stages (development, maturity, and dissipation) are essential for understanding precipitation dynamics. This study proposes a morphological precipitation event extraction (MPEE) method and a lifecycle fitting model, applied to CONUS404, Integrated Multi-satellitE Retrievals for GPM, and ECMWF Reanalysis 5 from 2001 to 2021. Intercomparison results confirm the method's robustness, with most correlation coefficients exceeding 0.5 and most root mean squared errors less than 0.7 mm/hr, between extracted events and simulated life cycles. K-means clustering reveals four precipitation types: common, high-peak, long-duration, and slow-developing events with delayed peaks. The method effectively captures precipitation variability across data sets and provides a scalable approach for studying long-term precipitation trends. This work lays a foundation for analyzing climate-scale precipitation lifecycle changes, improving our understanding of precipitation dynamics and their implications for climate variability.

**Plain Language Summary** Precipitation is a vital part of the Earth's water cycle, but tracking and understanding how rain events form, grow, and fade is challenging. This study introduces a new method to identify and analyze precipitation events over the U.S. using a shape-based technique. By applying this approach to three different rainfall data sets, the study finds that it reliably captures rainfall patterns and helps distinguish different types of precipitation events. The method also provides insights into how rainfall behaves over time, which can improve climate studies and weather predictions. Despite some limitations in capturing small or complex events, this research offers a valuable tool for studying long-term precipitation trends and understanding the effects of climate change on rainfall.

## 1. Introduction

Precipitation is one of the most essential components of the ecosystem and serves as a key driver of both the global water cycle and energy circulation (Feng et al., 2016; Huffman et al., 2015; Zhu & Ma, 2022). While precipitation events naturally evolve continuously in space and time, most studies analyze precipitation on a pixel-by-pixel basis, neglecting the spatial and temporal interconnections between pixels (Li et al., 2022; Tang et al., 2016; Zhu et al., 2021). This limitation hinders an integrated and comprehensive understanding of the precipitation lifecycle and its responses to climate change. To address this gap, it is essential to develop advanced methods that can effectively extract precipitation events from gridded precipitation data sets and capture precipitation lifecycle stages (development, maturity, and dissipation) (McAnelly & Cotton, 1989; Prein et al., 2017). However, this task remains challenging due to the complexity in precipitation processes and data sets.

The development of object-based precipitation extraction methods has evolved from static identification to dynamic tracking, continuously improving the ability to capture the spatiotemporal continuity of precipitation systems (Laverde-Barajas et al., 2019; Zahraei et al., 2013). Davis et al. (2006a, 2006b) developed the Method for Object-based Diagnostic Evaluation (MODE), which defined precipitation objects as contiguous rainy areas and

**Writing – original draft:** Siyu Zhu, Guoqiang Tang, Yu Du, Mofan Zhang, Mengye Chen, Huan Li, Yang Hong
**Writing – review & editing:** Siyu Zhu, Guoqiang Tang, Yu Du, Mofan Zhang, Mengye Chen, Huan Li, Yang Hong

was applied to analyze mesoscale precipitation events. Later advancements incorporated the temporal dimension, allowing for the tracking of precipitation system lifecycles, such as the improvements made to MODE by Skok et al. (2009, 2010), and further refinements by Skok et al. (2013) to optimize the identification of tropical cyclones by decomposing full 3D objects into smaller components. To enhance tracking accuracy, Clark et al. (2014) introduced the MODE Time Domain (MTD) method, which integrated lifecycle tracking of precipitation systems, a technique later refined by Ayat, Evans, and Behrangi (2021) and Ayat, Evans, Sherwood, and Behrangi (2021) to account for splitting and merging effects in precipitation systems. Nevertheless, recent applications have revealed that even the enhanced MTD framework still suffers from several practical limitations. For example, Li et al. (2023) showed that MTD's fixed-threshold segmentation tends to fragment rapidly evolving convective clusters during the re-intensification of Hurricane Florence, whereas R. Li et al. (2025) demonstrated that MTD may mis-represent the life-cycle-dependent error patterns of multi-satellite precipitation products because of its sensitivity to object splitting and temporal overlap. These studies highlight the need for event-extraction approaches that are less threshold-dependent and can more faithfully capture the complete evolution of both large and small precipitation systems.

More recently, researchers have employed increasingly flexible tracking approaches, such as Cui et al. (2020) using the Flexible Object Tracker (FLEXTRKR) method (Feng et al., 2018) to study mesoscale convective systems (MCSs), and Li et al. (2015, 2016) applying the watershed transformation to identify precipitation objects. Zhou et al. (2019) introduced the recursive-fractal approach, leveraging Integrated Multi-satellitE Retrievals for GPM (IMERG) data to extract extreme precipitation events. These advancements demonstrate that object-based methods provide a more comprehensive understanding of the evolution of precipitation systems. While object-based tracking methods have significantly advanced precipitation analysis, most existing approaches focus on extreme precipitation events, MCSs, or large-scale precipitation systems (Wang et al., 2023). However, given the transient characteristics, elevated noise levels, and frequent merging or fragmentation of small-scale precipitation, current methods still require methodological refinement to accurately identify and track smaller events.

In recent years, research leveraging event extraction methods to study precipitation lifecycles has gained momentum, offering insights beyond traditional statistical analyses for climate change studies and disaster management. Roca et al. (2020) highlight that in tropical regions, precipitation systems exhibit complex life cycles that directly influence local weather patterns, resource availability, and ecosystem health, underscoring the need to incorporate lifecycle dynamics into climate studies. Similarly, Hirata and Grimm (2016) demonstrate that atmospheric anomalies play a crucial role in shaping extreme rainfall events, making lifecycle analysis vital for predicting and mitigating risks such as flooding and droughts. Almazroui et al. (2012) show that modeling the lifecycle of extreme rainfall events helps explain temporal and spatial rainfall variability, offering practical insights for urban planning and disaster risk management. Additionally, Post and Knapp (2020) emphasize the role of precipitation timing and intensity in ecological processes, particularly in semi-arid regions, where understanding precipitation lifecycles supports water management and sustainability efforts. However, the automatic determination of lifecycle analysis for various precipitation events remains challenging today, as it heavily depends on the quality of extracted precipitation events and is constrained by the complexity of diverse precipitation patterns.

Motivated by a detailed analysis of precipitation event lifecycles, this study aims to (a) develop a novel morphological precipitation event extraction (MPEE) method that utilizes 3D connected domain identification to better capture the spatial and temporal evolution of precipitation systems; (b) propose a lifecycle fitting model that represents precipitation evolution through a parameterized curve encompassing development, maturity, and dissipation stages, providing a generalized framework for automatically deriving precipitation dynamics; (c) analyze the typical precipitation patterns over CONUS based on the framework with three distinct precipitation sources. This study has the great potential on deepening the understanding of precipitation variability and lays a foundation for climate-scale precipitation research.

## 2. Precipitation Data Sets

### 2.1. CONUS404

The four-km long-term regional hydroclimate reanalysis over the conterminous United States (CONUS404) data set, developed collaboratively by the National Center for Atmospheric Research and the U.S. Geological Survey

(USGS), is a high-resolution (4 km) hydroclimate reanalysis product spanning over 40 years (October 1979 to September 2021) (Rasmussen et al., 2023). CONUS404 data is publicly accessible and could be downloaded at https://rda.ucar.edu/datasets/d559000/.

### 2.2. IMERG

Integrated Multi-satellitE Retrievals for GPM (IMERG) was developed based on the TRMM mission, which laid the foundation for retrieving precipitation data from space based on multisource remote sensing data (Huffman et al., 2015, 2020; Zhu, Li, Chen, Wen, Liu, et al., 2024). IMERG is a state-of-the-art precipitation data set widely used in rainfall analysis, climate studies, and hydrological modeling, providing high-resolution, globally consistent precipitation estimates (Zhu, Li, Chen, Wen, Gao, et al., 2024, Zhu, Li, Chen, Wen, Liu, et al., 2024). In this study, the Final run of IMERG version seven is used to extract the precipitation events (Huffman et al., 2022). The IMERG could be downloaded at https://gpm.nasa.gov/data/imerg.

### 2.3. ERA5

Produced by the European Centre for Medium-Range Weather Forecasts (ECMWF), ECMWF Reanalysis 5 (ERA5) represents a state-of-the-art reanalysis data set offering high-resolution global atmospheric and oceanic information (Hersbach et al., 2020). In this study, ERA5 data, originally at 0.25-degree and hourly resolution, is resampled to 0.1-degree resolution using bilinear interpolation to ensure consistency with the other data sets. Additionally, ERA5 data could be accessed at https://www.ecmwf.int/en/forecasts/dataset/ecmwf-reanalysis-v5.

In this study, CONUS404, IMERG, and ERA5 were chosen primarily because they each provide at least 20 consecutive years of continuous data spanning from 2001 to 2021 (details in Table S1 in Supporting Information S1), because long-term data is crucial to capturing precipitation variability and studying climate impacts. Additionally, CONUS404 provides other essential atmospheric and land surface variables beyond precipitation, facilitating a deeper understanding of the physical mechanisms behind precipitation events. Therefore, the combination of CONUS404, IMERG, and ERA5 enables a comprehensive and consistent investigation of precipitation lifecycle characteristics over both weather and climate timescales.

## 3. Methodology

### 3.1. Three-Dimensional Morphological Extraction of Precipitation Events

We develop a novel MPEE algorithm for extracting the precipitation events at the three-dimensional scale. The method includes four main steps:

1. Smoothing the data: A 5 × 5 × 5 (latitude, longitude and time) mean filter is applied to smooth the precipitation data by averaging values within a spatiotemporal window. This reduces local noise and prevents small fluctuations from affecting event detection. Without smoothing, scattered noise could introduce artificial precipitation events or break up continuous ones, leading to inaccurate identification.
2. Determining the precipitation events: Pixels with values greater than a precipitation threshold (Pthd) are classified as precipitation pixels (marked as 1), while all other pixels are marked as 0. Without this threshold, tiny precipitation grids may create spurious connections between separate precipitation events, leading to overestimated event sizes.
3. Searching for seeds: Seeds for extreme precipitation events are identified by selecting grid points where the smoothed precipitation pixels exceed the seed threshold (Sthd). These are determined using connected component labeling and serve as the initial points for event detection and region growing. The choice of Sthd is a key parameter in the calibration process, as it directly impacts how precipitation events are defined and distinguished from each other.
4. Iteratively calculating for matching the whole precipitation events: The seed pixels are expanded iteratively using a 3D morphological dilation process. A spherical structuring element is applied to dilate the core regions, gradually incorporating neighboring pixels marked as precipitation pixels in step 2. This process continues for a specified number of iterations (Buffer Number), ensuring that precipitation pixels connected to the growing event are assigned to the same precipitation event.

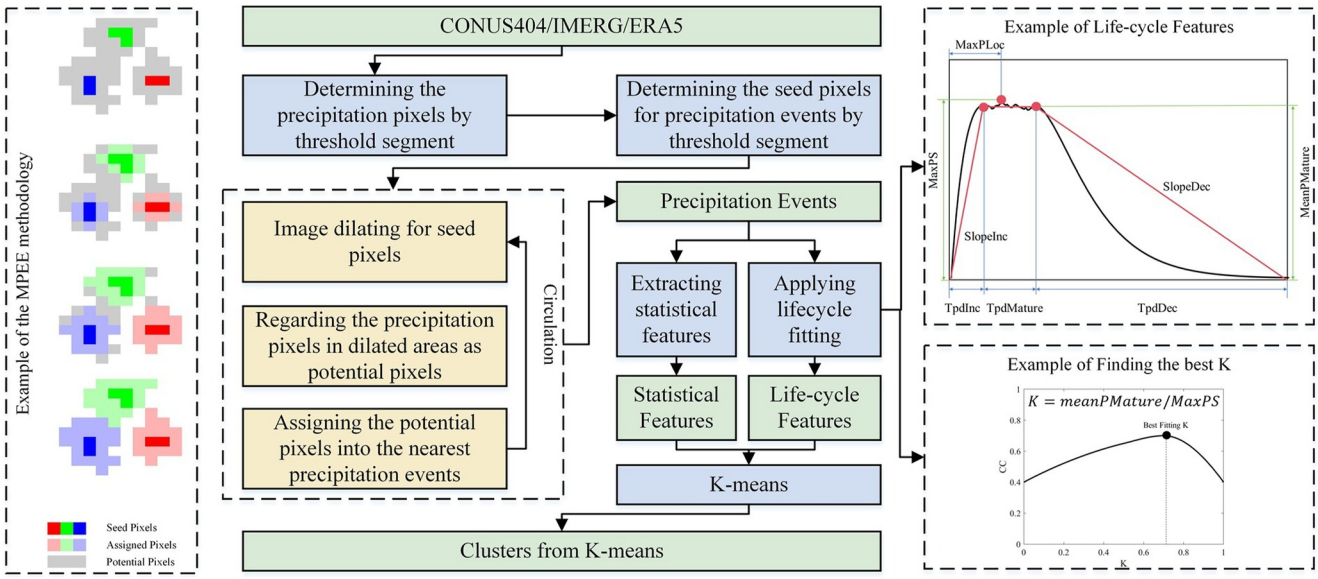


**Figure 1.** The Structure of morphological precipitation event extraction and corresponding lifecycle model. The precipitation lifecycle features include maximum precipitation (MaxPS), mean precipitation of mature stage (MeanPMature), the timing of MaxPS (MaxPLoc), slope of increasing stage (SlopeInc), slope of decreasing stage (SlopeDec), the time period of increasing stage (TpdInc), the time period of mature stage (TpdMature), and the time period of decreasing stage (TpdDec).

Finally, discrete precipitation events are generated with all relevant precipitation pixels mapped to those events accordingly. Additionally, the parameter calibration details are provided (details in Figures S1 to S4 in Supporting Information S1), with Pthd, Sthd, and Buffer Number assigned as 0.1 mm/hr, 1.5 mm/hr and 50, respectively.

### 3.2. The Lifecycle Model for Precipitation Event

The input data of this study include CONUS404, IMERG and ERA5, which are all clipped to the range of CONUS (from 130° to 60°W, and from 20° to 55°N) because it contains various climate zones (Zhu, Li, Chen, Wen, Gao, et al., 2024). Based on the extracted precipitation events, the lifecycle is calculated by averaging precipitation values at each time step (hourly in this study). We hypothesize that the lifecycle of a common precipitation event consists of three phases: development, maturity, and dissipation (Figure 1), which can be represented by a trapezoidal curve (with time on the *x*-axis and precipitation intensity on the *y*-axis). The development and dissipation phases occur before and after the mature phase, respectively, and are characterized by linear increases and decreases in precipitation. The mature phase, represented by a horizontal line of variable length, has a y-value equal to the maximum precipitation (MaxPS) value multiplied by the mature coefficient (K, which means the precipitation of mature stage divided the MaxPS). This coefficient is determined through an optimization process, where the simulated curve achieves the maximum correlation coefficient (CC) with the actual precipitation curve. Although this simulated curve does not represent all precipitation events, it effectively characterizes typical events with clear development, maturity, and dissipation phases. Using this model, we can describe the lifecycle of a precipitation event and calculate its corresponding lifecycle characteristics. The relevant lifecycle characteristic calculations are shown in Equations 1–3.

$$K = meanPMature/MaxPS \tag{1}$$

$$SlopeInc = meanPMature/TpdInc \tag{2}$$

$$SlopeDec = meanPMature/DecInc \tag{3}$$

where *meanPMature* and *MaxPS* represent the average precipitation value in mature stage and the MaxPS value, respectively; meanwhile *SlopeInc* and *SlopeDec* denote the slopes of development and dissipation stages, respectively; similarly, *TpdInc* and *DecInc* are the period lengths of development and dissipation stages, respectively; and the *K* is the mature ratio.

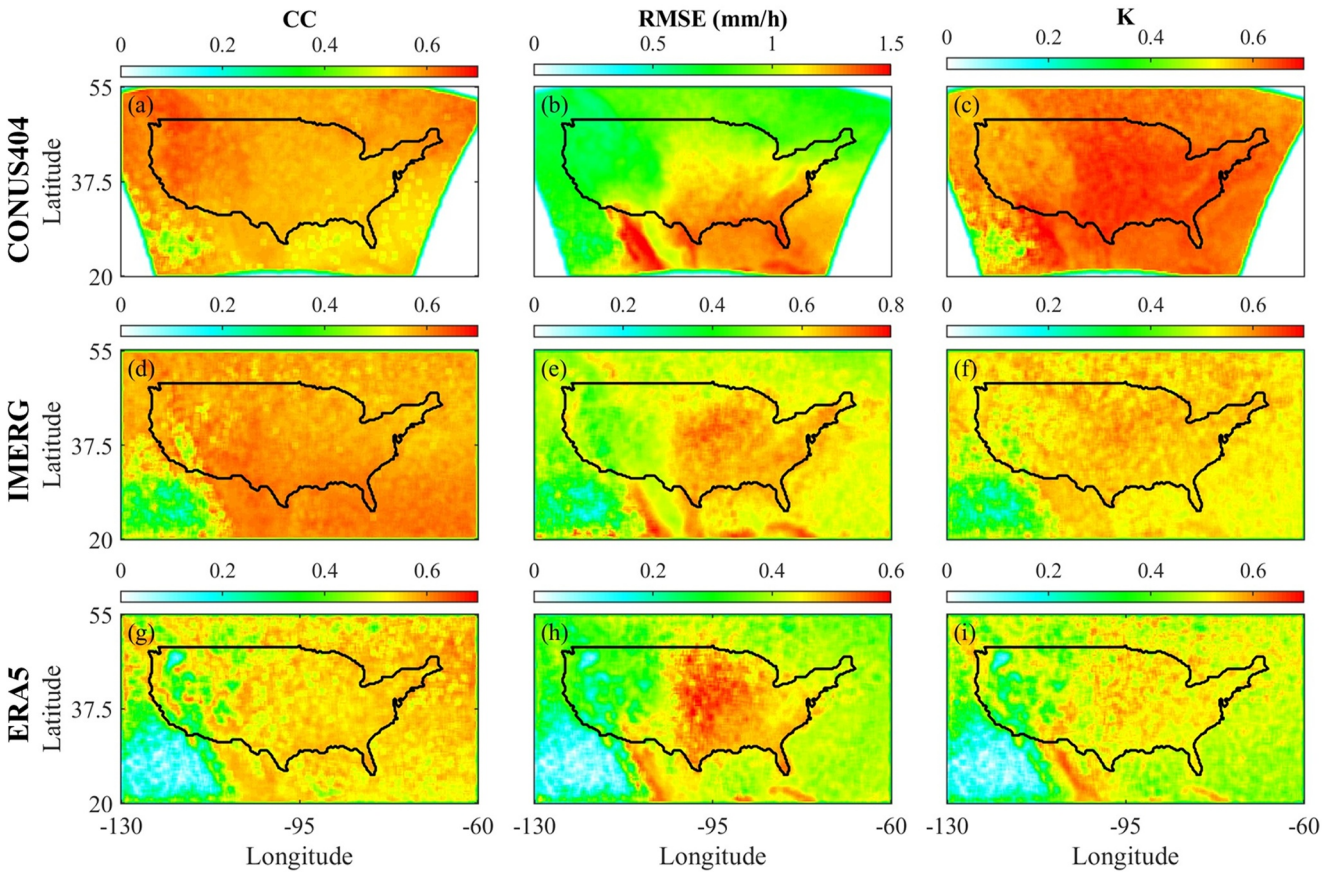


**Figure 2.** Spatial distribution of evaluation metrics for the lifecycle model. Each row represents a different data set: (a–c) CONUS404, (d–f) Integrated Multi-satellitE Retrievals for GPM, and (g–i) ECMWF Reanalysis 5. Each column represents a different evaluation metric: (a, d, g) correlation coefficient (CC), (b, e, h) root mean squared error (RMSE, mm/h), and (c, f, i) maturity coefficient (K).

### 3.3. Intercomparison

Since precipitation event extraction is a complex and abstract process, it is challenging to establish standard evaluation metrics or ground truth data (Wang et al., 2023; Wang & Tang, 2020). To assess performance, we compare the simulated curves generated from the lifecycle model with the recorded curves from the input data sets (CONUS404, IMERG, and ERA5), providing an indirect validation of the method. Additionally, we conduct intercomparison by applying the same extraction method and lifecycle analysis across these three data sets and comparing the results. If the extracted precipitation events and lifecycle characteristics show consistency across data sets, it strengthens the reliability and robustness of MPEE. To intercompare the K-means results, we used eight lifecycle features, including SlopeInc, MeanPMature, SlopeDec, TpdMature, K, KTpd, MaxPS, and Duration ($D$), all of which were normalized before clustering, and which represent the slope of the increasing stage, mean precipitation during the mature stage, slope of the decreasing stage, time period of the mature stage, maturity coefficient, the ratio of mature time to the total duration, MaxPS, and overall duration, respectively.

## 4. Results

### 4.1. The Evaluation of the Lifecycle Model for Precipitation Events

As shown in Figure 2, these data sets all show high CC (~0.6) over CONUS, demonstrating that the lifecycle model is capable of capturing the main trends of the precipitation events (case studies in Figures S5 and S6 in Supporting Information S1). By further examining the spatial distribution of events whose fitted curves achieve CC > 0.6 (see Figure S7 in Supporting Information S1), we find that the pattern of these high-skill events closely mirrors that of the total event population (with a larger concentration over the southern coastal/oceanic sector), indicating that the model does not introduce any appreciable geographic bias in representing precipitation

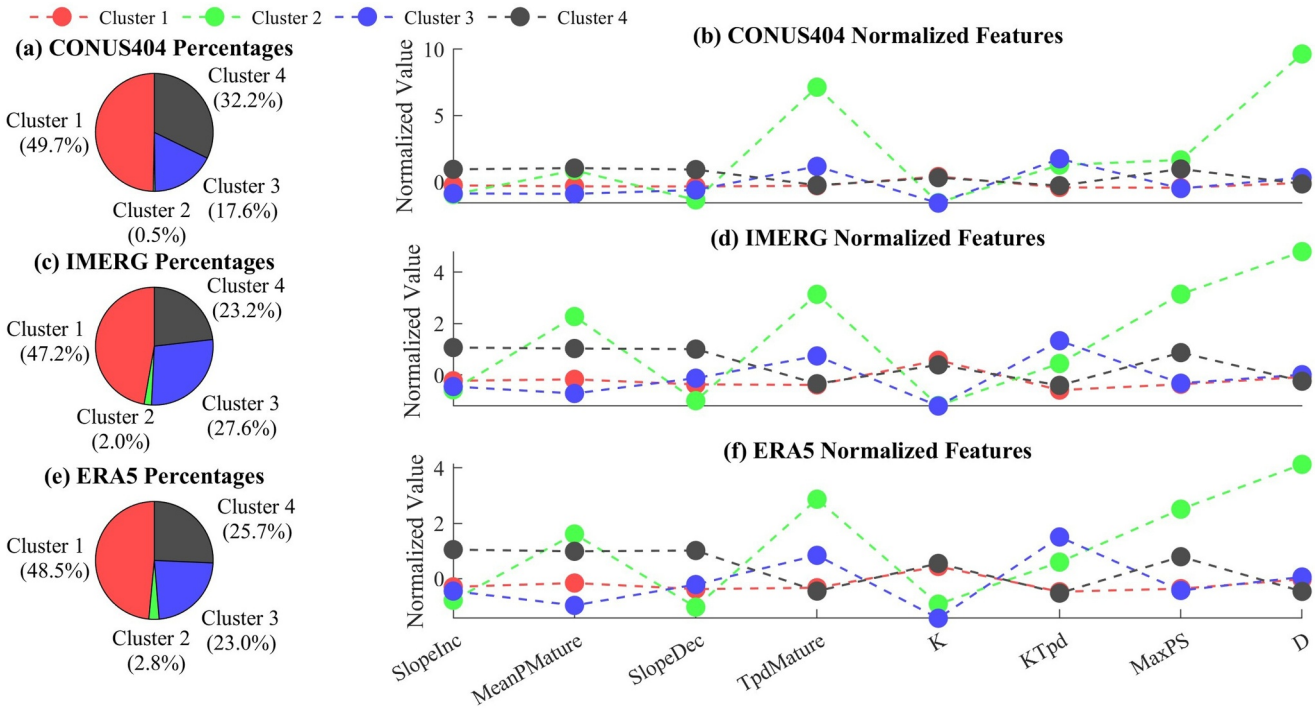


**Figure 3.** The results of K-means including (left panel) the pie figure to show the percentages of different clusters and (right panel) the normalized values of various lifecycle features, based on (a–b) CONUS404, (c–d) Integrated Multi-satellitE Retrievals for GPM, and (e–f) ECMWF Reanalysis 5. Here SlopeInc, MeanPMature, SlopeDec, TpdMature, K, KTpd, maximum precipitation (MaxPS) and D represent the slope of increasing stage, mean precipitation of mature stage, slope of decreasing stage, time period of mature stage, mature coefficient, the ratio of mature time to the total duration, MaxPS and duration, respectively.

lifecycles. Although the lifecycle model may not perform as well in the southwestern part of the study region, where the CC is below 0.3, this could be attributed to several factors. One reason may be the relatively low precipitation in this area, combined with the more complex and rapid evolution of precipitation events. Additionally, boundary limitations of the interested region may prevent the extraction of complete lifecycle events, as some precipitation systems could enter from the edges of the domain. For root mean squared error (RMSE), the results from the three data sets show similar spatial patterns across CONUS. The central and eastern regions exhibit higher RMSE values compared to the western region, indicating greater precipitation variability in these areas, making it more challenging to capture with a simple lifecycle pattern. For the coefficient K, CONUS404 shows relatively higher values compared to IMERG and ERA5, which may be attributed to differences in spatial resolution and projection. This is supported by the similarity in the spatial patterns of K between IMERG and ERA5, although K of IMERG is overall higher than that of ERA5.

### 4.2. The Typical Types of Curves Based on K-Means Classification

To demonstrate the applicability of our model in distinguishing different precipitation event patterns, we applied the K-means clustering algorithm, an unsupervised classification method, to identify distinct lifecycle characteristics. Based on the Elbow method, four clusters were identified as the most suitable, as the within-cluster sum of squared errors (WCSS) shows a clear inflection point at this number, indicating minimal gain from additional clusters. These clusters were then applied to the CONUS404, IMERG, and ERA5 data sets, as shown in Figure 3. The results indicated that all data sets exhibited similar proportions across the clusters, with Cluster 1 to Cluster 4 representing approximately 48%, 2%, 23%, and 27% of the events, respectively.

The lifecycle features of the corresponding clusters also displayed similar patterns across all data sets. Cluster 1 represents the most common type of precipitation event, with features mostly centered around the mean. Cluster 2 captures events that last significantly longer, characterized by extreme values for Duration ($D$) and relatively higher MaxPS. Cluster 3 is defined by low K and high KTpd, indicating slower development and dissipation, with an extended mature phase. Cluster 4 is characterized by steep SlopeInc and SlopeDec, along with relatively high

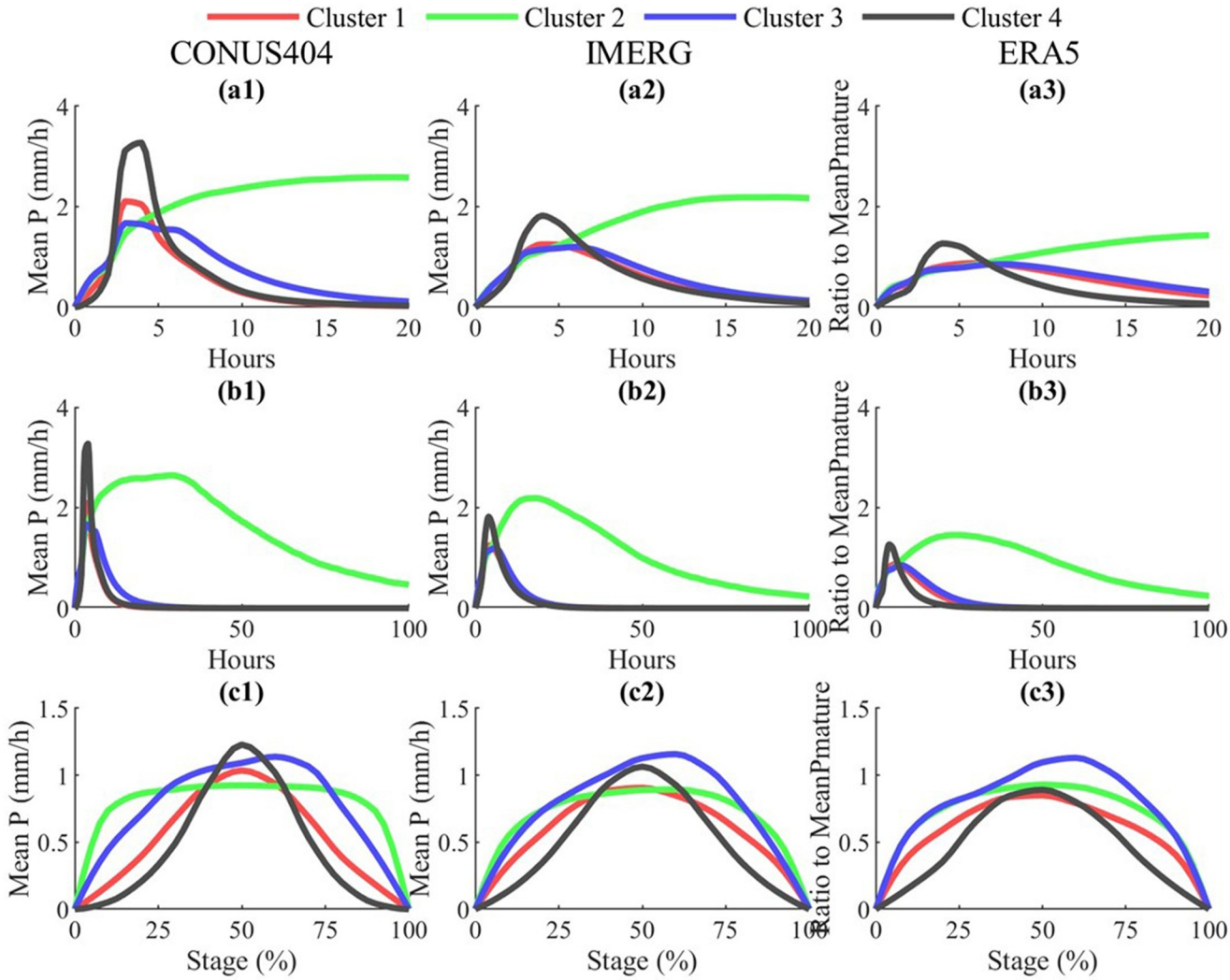


**Figure 4.** The curve performances of different clusters from K-means in terms of (a) the curve shapes in range from 0 to 20 hr, (b) the curve shapes in range from 0 to 100 hr, and (c) the normalized curve shapes by taking *x* as percentage stages and taking *y* as the normalized precipitation (which value is divided by the precipitation at the mature stage). Note that the columns 1 to 3 represent the CONUS404, Integrated Multi-satellitE Retrievals for GPM and ECMWF Reanalysis 5, respectively.

MaxPS, reflecting rapid development and dissipation, typical of intense convective rain events. This clustering approach provides a clear understanding of the different types of precipitation events across these data sets.

### 4.3. The Typical Curves of Different Clusters Based on K-Means

Analyzing the feature distributions of these clusters alone is insufficient to fully uncover their differences. Therefore, we averaged the curves within each cluster, using both real hours and the percentage of each lifecycle stage on the *x*-axis to gain deeper insights (Figure 4). It is clear that Cluster 2 differs significantly from the other clusters, as its lifecycle extends for more than 100 hr, with the mature stage lasting around 20–30 hr. In contrast, the mature stage for the other clusters is only around 3–5 hr. On the hourly axis (Figures 4a and 4b), Cluster 1 and Cluster 3 exhibit similar shapes. However, compared to Cluster 1, Cluster 3 has a longer mature stage and a lower peak precipitation value. Cluster 4, on the other hand, shows a much higher peak precipitation value compared to both Cluster 1 and Cluster 3. Correspondingly, the rates of change during the development and dissipation stages in Cluster 4 are also faster. From this, we can conclude that Cluster 4 experiences the fastest lifecycle changes among the clusters, while Cluster 2 has the slowest and longest lifecycle.

We also averaged the ratios relative to MeanPMature as the *y*-axis, using the percentage of each lifecycle stage as the *x*-axis. This approach, instead of relying on an hourly scale, allows us to more clearly distinguish between the previously hard-to-differentiate Cluster 1 and Cluster 3. As shown in Figure 4c, Cluster 3 and Cluster 4 display flatter curves, indicating that the mature stage dominates the majority of their lifecycle, occupying over 50%. In contrast, the mature stage for Cluster 1 and Cluster 2 accounts for only about 15%–25% of the lifecycle. Another notable characteristic of Cluster 2 is that its peak precipitation value tends to occur later in the lifecycle, around 60%–70%, whereas the other clusters reach their peak near the middle, around 50%. In Cluster 2, precipitation develops slowly, the mature stage is prolonged, but after reaching the peak, it dissipates quickly. The MPEE and lifecycle model robustly identify and classify precipitation events across multiple data sets, demonstrating high consistency and reliability.

## 5. Discussion

### 5.1. Advantages and Improvements of MPEE

Traditional object-based precipitation extraction methods, such as CRA, MODE, and MTD, primarily rely on the spatial connectivity of precipitation pixels to identify and track precipitation systems (Clark et al., 2014; Davis et al., 2006a). These methods, though effective for large systems, often over-aggregate small- and medium-scale events by merging adjacent grid cells based on threshold exceedance, even when connections are weak or artificial. However, the MPEE method uses a seed-based strategy with the 3D morphological dilation to identify core precipitation regions first, ensuring only nearby pixels are aggregated, thereby reducing false merging and improving event separation. As a result, MPEE enhances the physical realism of extracted events and improves the model's applicability to a broader spectrum of precipitation regimes, particularly those dominated by fragmented or intermittent rainfall.

### 5.2. Discussion About the Universality of the Lifecycle Model

While the proposed lifecycle model simplifies the evolution of precipitation events into three distinct stages (development, maturity, and dissipation), this segmentation inevitably overlooks certain complexities observed in real-world systems. For instance, some convective or tropical systems exhibit re-intensification, where precipitation intensity increases again after initial weakening. Our current model, based on a trapezoidal fit to identify the most correlated representation of the observed curve, does not capture such nonlinear behaviors. As a result, re-intensifying systems are either poorly fitted or excluded based on low correlation thresholds.

Furthermore, the simulated mature phase is derived by maximizing CC between the fitted and actual curves, with the maturity coefficient (K) defined as the ratio of mature-stage precipitation to the maximum event precipitation. This curve-fitting strategy enables objective lifecycle representation across diverse events but is not intended to universally replicate all precipitation systems. It serves as a generalized and scalable approximation that holds for the majority of events with clear peak structures. The inherent simplification, however, means that systems with multiple peaks or atypical evolution may not be well represented.

### 5.3. Inconsistency in Spatial Distribution of Precipitation Events

Additionally, we observe in Figure 2 that the RMSE distribution closely follows the spatial pattern of precipitation magnitude—lower in the West and higher in the East, particularly along coastal zones. This reflects a common characteristic in model evaluations where RMSE tends to be positively correlated with precipitation intensity. Therefore, we recommend using correlation-based metrics such as CC in tandem with RMSE to provide a more normalized and scale-invariant assessment of model performance. These considerations highlight the trade-offs between model generality and event-specific accuracy, and underscore the need for continued development of lifecycle modeling frameworks that balance robustness and flexibility.

## 6. Conclusion

In this study, we propose a novel MPEE method along with a lifecycle fitting model, designed to extract precipitation events using three-dimensional morphological theory and identify an optimal lifecycle curve for each event. To evaluate the performance of our algorithm, we calculate CC and RMSE between the extracted

precipitation events and the simulated lifecycle curves, while also applying intercomparison using data from CONUS404, IMERG, and ERA5. The main findings of this study can be summarized as follows:

1. Over CONUS, the CCs between the extracted precipitation events and the simulated lifecycle curves consistently reach 0.6 or higher, while the RMSE remains below 0.7 mm/hr in most cases, demonstrating the model's effectiveness in accurately capturing precipitation events.
2. The K-means clustering results reveal significant similarities in both the proportion of clusters and the distribution of lifecycle characteristics across the multi-source precipitation products (CONUS404, IMERG, and ERA5), demonstrating the robustness of our method.
3. The K-means clustering identifies four characteristic types of precipitation events: common and normal events, those with high peak values, those with long durations, and those with gentler development slopes, where the peak occurs significantly beyond 50% of the lifecycle.

This study provides a robust and scalable framework for identifying and characterizing precipitation events across multiple data sets using morphological theory and lifecycle modeling. It also lays a foundation for long-term lifecycle analysis, enhancing our understanding of climate change impacts on precipitation dynamics.

## Ethics Statements

This study contains no human subjects, human data or tissue, or animals.

## Conflict of Interest

The authors declare no conflicts of interest relevant to this study.

## Data Availability Statement

In this study, the IMERG, CONUS, and ERA5 data sets are utilized to extract precipitation events and conduct lifecycle analysis. The IMERG daily Version 06 Final Run data can be downloaded from the NASA official website at Huffman et al. (2015). The CONUS data can be downloaded from Rasmussen et al. (2023). The ERA5 data set could be downloaded at Hersbach et al. (2020). The MPEE algorithm and related materials (version 1.0.0) have been archived in Zenodo at Zhu et al. (2025). This version corresponds to the implementation used in the present study and aims to support long-term accessibility and reproducibility. The code is released under the MIT License and is also available for continued development at https://github.com/SiyuZhu2023/PrecipitationEventExtraction.

**Acknowledgments**
This study is supported by the National Natural Science Foundation of China (U2340213) and the University of Oklahoma Hydrology and Water Security Program.

## References

Almazroui, M., Nazrul Islam, M., Athar, H., Jones, P., & Rahman, M. A. (2012). Recent climate change in the Arabian Peninsula: Annual rainfall and temperature analysis of Saudi Arabia for 1978-2009. *International Journal of Climatology*, *32*(6), 953–966. https://doi.org/10.1002/joc.3446

Ayat, H., Evans, J. P., & Behrangi, A. (2021). How do different sensors impact IMERG precipitation estimates during hurricane days? *Remote Sensing of Environment*, *259*, 112417. https://doi.org/10.1016/j.rse.2021.112417

Ayat, H., Evans, J. P., Sherwood, S., & Behrangi, A. (2021). Are storm characteristics the same when viewed using merged surface radars or a merged satellite product? *Journal of Hydrometeorology*, *22*(1), 43–62. https://doi.org/10.1175/jhm-d-20-0187.1

Clark, A. J., Bullock, R. G., Jensen, T. L., Xue, M., & Kong, F. (2014). Application of object-based time-domain diagnostics for tracking precipitation systems in convection-allowing models. *Weather and Forecasting*, *29*(3), 517–542. https://doi.org/10.1175/waf-d-13-00098.1

Cui, W., Dong, X., Xi, B., Feng, Z., & Fan, J. (2020). Can the GPM IMERG final product accurately represent MCSs' precipitation characteristics over the central and eastern United States? *Journal of Hydrometeorology*, *21*(1), 39–57. https://doi.org/10.1175/jhm-d-19-0123.1

Davis, C., Brown, B., & Bullock, R. (2006a). Object-based verification of precipitation forecasts. Part I: Methodology and application to mesoscale rain areas. *Monthly Weather Review*, *134*(7), 1772–1784. https://doi.org/10.1175/mwr3145.1

Davis, C., Brown, B., & Bullock, R. (2006b). Object-based verification of precipitation forecasts. Part II: Application to convective rain systems. *Monthly Weather Review*, *134*(7), 1785–1795. https://doi.org/10.1175/mwr3146.1

Feng, Z., Leung, L. R., Hagos, S., Houze, R. A., Burleyson, C. D., & Balaguru, K. (2016). More frequent intense and long-lived storms dominate the springtime trend in central US rainfall. *Nature Communications*, *7*(1), 13429. https://doi.org/10.1038/ncomms13429

Feng, Z., Leung, L. R., Houze Jr, R. A., Hagos, S., Hardin, J., Yang, Q., et al. (2018). Structure and evolution of mesoscale convective systems: Sensitivity to cloud microphysics in convection-permitting simulations over the United States. *Journal of Advances in Modeling Earth Systems*, *10*(7), 1470–1494. https://doi.org/10.1029/2018ms001305

Hersbach, H., Bell, B., Berrisford, P., Hirahara, S., Horányi, A., Muñoz-Sabater, J., et al. (2020). The ERA5 global reanalysis [Dataset]. *Quarterly Journal of the Royal Meteorological Society*, *146*, 1999–2049. https://doi.org/10.24381/cds.adbb2d47

Hirata, F. E., & Grimm, A. M. (2016). The role of synoptic and intraseasonal anomalies in the life cycle of summer rainfall extremes over South America. *Climate Dynamics*, *46*(9–10), 3041–3055. https://doi.org/10.1007/s00382-015-2751-6

Huffman, G., Bolvin, D., Nelkin, E., & Tan, J. (2022). *On the Verge of IMERG Version 07*. Authorea Preprints. https://doi.org/10.1002/essoar.10510208.1

Huffman, G. J., Bolvin, D. T., Braithwaite, D., Hsu, K., Joyce, R., Xie, P., & Yoo, S.-H. (2015). NASA global precipitation measurement (GPM) integrated multi-satellite retrievals for GPM (IMERG) [Dataset]. *Algorithm theoretical basis document version*, *4*, 30. https://doi.org/10.5067/GPM/IMERGDF/DAY/06

Huffman, G. J., Bolvin, D. T., Braithwaite, D., Hsu, K.-L., Joyce, R. J., Kidd, C., et al. (2020). Integrated multi-satellite retrievals for the global precipitation measurement (GPM) mission (IMERG). *Satellite Precipitation Measurement*, 343–353. https://doi.org/10.1007/978-3-030-24568-9_19

Laverde-Barajas, M., Corzo, G., Bhattacharya, B., Uijlenhoet, R., & Solomatine, D. P. (2019). Spatiotemporal analysis of extreme rainfall events using an object-based approach. In *Spatiotemporal analysis of extreme hydrological events* (pp. 95–112). Elsevier.

Li, J., Hsu, K., AghaKouchak, A., & Sorooshian, S. (2015). An object-based approach for verification of precipitation estimation. *International Journal of Remote Sensing*, *36*(2), 513–529. https://doi.org/10.1080/01431161.2014.999170

Li, J., Hsu, K.-L., AghaKouchak, A., & Sorooshian, S. (2016). Object-based assessment of satellite precipitation products. *Remote Sensing*, *8*(7), 547. https://doi.org/10.3390/rs8070547

Li, R., Guilloteau, C., Kirstetter, P.-E., & Foufoula-Georgiou, E. (2025). Understanding the error patterns of multi-satellite precipitation products during the lifecycle of precipitation events for diagnostics and algorithm improvement. *Journal of Hydrology*, *651*, 132610. https://doi.org/10.1016/j.jhydrol.2024.132610

Li, Z., Tang, G., Kirstetter, P., Gao, S., Li, J.-L., Wen, Y., & Hong, Y. (2022). Evaluation of GPM IMERG and its constellations in extreme events over the conterminous United States. *Journal of Hydrology*, *606*, 127357. https://doi.org/10.1016/j.jhydrol.2021.127357

Li, Z., Tiwari, A., Sui, X., Garrison, J., Marks, F., & Niyogi, D. (2023). Studying Brown ocean Re-intensification of hurricane florence using CYGNSS and SMAP soil moisture data and a numerical weather model. *Geophysical Research Letters*, *50*(19), e2023GL105102. https://doi.org/10.1029/2023gl105102

McAnelly, R. L., & Cotton, W. R. (1989). The precipitation life cycle of mesoscale convective complexes over the central United States. *Monthly Weather Review*, *117*(4), 784–808. https://doi.org/10.1175/1520-0493(1989)117<0784:tplcom>2.0.co;2

Post, A. K., & Knapp, A. K. (2020). The importance of extreme rainfall events and their timing in a semi-arid grassland. *Journal of Ecology*, *108*(6), 2431–2443. https://doi.org/10.1111/1365-2745.13478

Prein, A. F., Liu, C., Ikeda, K., Trier, S. B., Rasmussen, R. M., Holland, G. J., & Clark, M. P. (2017). Increased rainfall volume from future convective storms in the US. *Nature Climate Change*, *7*(12), 880–884. https://doi.org/10.1038/s41558-017-0007-7

Rasmussen, R., Liu, C., Ikeda, K., Chen, F., Kim, J.-H., Schneider, T., et al. (2023). Four-kilometer long-term regional hydroclimate reanalysis over the conterminous United States (CONUS) [Dataset]. *Research Data Archive at the National Center for Atmospheric Research, Computational and Information Systems Laboratory*. https://doi.org/10.5065/ZYY0-Y036

Roca, R. m., Bouniol, D., & Fiolleau, T. (2020). On the duration and life cycle of precipitation systems in the tropics. In *Satellite Precipitation Measurement* (Vol. 2, pp. 729–744). Springer. https://doi.org/10.1007/978-3-030-35798-6_14

Skok, G., Bacmeister, J., & Tribbia, J. (2013). Analysis of tropical cyclone precipitation using an object-based algorithm. *Journal of Climate*, *26*(8), 2563–2579. https://doi.org/10.1175/jcli-d-12-00135.1

Skok, G., Tribbia, J., & Rakovec, J. (2010). Object-based analysis and verification of WRF model precipitation in the low-and midlatitude Pacific Ocean. *Monthly Weather Review*, *138*(12), 4561–4575. https://doi.org/10.1175/2010mwr3472.1

Skok, G., Tribbia, J., Rakovec, J., & Brown, B. (2009). Object-based analysis of satellite-derived precipitation systems over the low-and mid-latitude Pacific Ocean. *Monthly Weather Review*, *137*(10), 3196–3218. https://doi.org/10.1175/2009mwr2900.1

Tang, G., Ma, Y., Long, D., Zhong, L., & Hong, Y. (2016). Evaluation of GPM Day-1 IMERG and TMPA Version-7 legacy products over Mainland China at multiple spatiotemporal scales. *Journal of Hydrology*, *533*, 152–167. https://doi.org/10.1016/j.jhydrol.2015.12.008

Wang, T., Li, Z., Ma, Z., Gao, Z., & Tang, G. (2023). Diverging identifications of extreme precipitation events from satellite observations and reanalysis products: A global perspective based on an object-tracking method. *Remote Sensing of Environment*, *288*, 113490. https://doi.org/10.1016/j.rse.2023.113490

Wang, T., & Tang, G. (2020). Spatial variability and Linkage between extreme convections and extreme precipitation revealed by 22-year space-borne precipitation radar data. *Geophysical Research Letters*, *47*(12), e2020GL088437. https://doi.org/10.1029/2020gl088437

Zahraei, A., Hsu, K.-l., Sorooshian, S., Gourley, J. J., Hong, Y., & Behrangi, A. (2013). Short-term quantitative precipitation forecasting using an object-based approach. *Journal of Hydrology*, *483*, 1–15. https://doi.org/10.1016/j.jhydrol.2012.09.052

Zhou, Y., Nelson, K., Mohr, K. I., Huffman, G. J., Levy, R., & Grecu, M. (2019). A spatial-temporal extreme precipitation database from GPM IMERG. *Journal of Geophysical Research: Atmospheres*, *124*(19), 10344–10363. https://doi.org/10.1029/2019jd030449

Zhu, S., Li, Z., Chen, M., Wen, Y., Gao, S., Zhang, J., et al. (2024). How has the latest IMERG V07 improved the precipitation estimates and hydrologic utility over CONUS against IMERG V06? *Journal of Hydrology*, *645*, 132257. https://doi.org/10.1016/j.jhydrol.2024.132257

Zhu, S., Li, Z., Chen, M., Wen, Y., Liu, Z., Huffman, G. J., et al. (2024). Evaluation of IMERG climate trends over land in the TRMM and GPM eras. *Environmental Research Letters*, *20*(1), 014064. https://doi.org/10.1088/1748-9326/ad984e

Zhu, S., & Ma, Z. (2022). PECA-FY4A: Precipitation Estimation using Chromatographic Analysis methodology for full-disc multispectral observations from FengYun-4A/AGRI. *Remote Sensing of Environment*, *282*, 113234. https://doi.org/10.1016/j.rse.2022.113234

Zhu, S., Ma, Z., Xu, J., He, K., Liu, H., Ji, Q., et al. (2021). A morphology-based adaptively spatio-temporal merging algorithm for optimally combining multisource gridded precipitation products with various resolutions. *IEEE Transactions on Geoscience and Remote Sensing*, *60*, 1–21. https://doi.org/10.1109/tgrs.2021.3097336

Zhu, S., Tang, G., Yan, S., Du, Y., Xu, Y., Zhang, M., et al. (2025). Morphological precipitation event extraction (MPEE) [version 1.0.0] [Software]. *Zenodo*. https://doi.org/10.5281/zenodo.15529577